Nanoscale

Epitaxial Graphene/Silicon Carbide Intercalation: A Minireview on Graphene Modulation and Unique 2D Materials

Journal:	*Nanoscale*
Manuscript ID	NR-MRV-05-2019-003721.R2
Article Type:	Minireview
Date Submitted by the Author:	27-Jul-2019
Complete List of Authors:	Briggs, Natalie; The Pennsylvania state university, Material Science and Engineering Gebeyehu, Zewdu ; Catalan Institute of Nanoscience and Nanotechnology; Barcelona Institute of Science and Technology; Universitat Autonoma de Barcelona; Pennsylvania State University, Materials Science & Engineering Vera, Alexander; Pennsylvania State University, Materials Science & Engineering Zhao, Tian; Pennsylvania State University, Chemistry Wang, Ke; The Pennsylvania State University, Materials Research Institute De La Fuente Duran, Ana; Pennsylvania State University, Materials Science & Engineering Bersch, Brian; Pennsylvania State University, Materials Science and Engineering Bowen, Timothy; Pennsylvania State University, Materials Science & Engineering Knappenberger, Kenneth; Penn State Department of Chemistry, Chemistry Department Robinson, J; The Pennsylvania State University,

Epitaxial Graphene/Silicon Carbide Intercalation: A Minireview on Graphene Modulation and Unique 2D Materials

Natalie Briggs[1,2,3], Zewdu M. Gebeyehu[1,4,5], Alexander Vera[1,2], Tian Zhao[6], Ke Wang[7], Ana De La Fuente Duran[1], Brian Bersch[1,2], Timothy Bowen[1,2], Kenneth L. Knappenberger, Jr.[6], Joshua A. Robinson[1,2,3,8]

[1]Department of Materials Science & Engineering, Pennsylvania State University, University Park, PA 16802
[2]Center for 2-Dimensional and Layered Materials, Pennsylvania State University, University Park, PA 16802
[3]2-Dimensional Crystal Consortium Materials Innovation Platform, Pennsylvania State University, University Park, PA 16802
[4]Catalan Institute of Nanoscience and Nanotechnology (ICN2), CSIC, The Barcelona Institute of Science and Technology (BIST), Campus UAB, Bellaterra, Spain, Barcelona, Spain
[5]Universitat Autònoma de Barcelona (UAB), Bellaterra, Spain
[6]Department of Chemistry, Pennsylvania State University, University Park, PA 16802
[7]Materials Characterization Laboratory, University Park, PA 16802
[8]Center for Atomically-Thin Multifunctional Coatings, Pennsylvania State University, University Park, PA 16802

Abstract

Intercalation of atomic species through epitaxial graphene on silicon carbide began only a few years following its initial report in 2004.[1] The impact of intercalation on the electronic properties of the graphene is well known; however, the intercalant itself can also exhibit intriguing properties not found in nature.[2] This realization has inspired new interest in epitaxial graphene/silicon carbide (EG/SiC) intercalation, where the scope of the technique extends beyond modulation of graphene properties to the creation of new 2D forms of 3D materials. The mission of this minireview is to provide a concise introduction to EG/SiC intercalation and to demonstrate a simplified approach to EG/SiC intercalation. We summarize the primary techniques used to achieve and characterize EG/SiC intercalation, and show that thermal evaporation-based methods can effectively substitute for more complex synthesis techniques, enabling large-scale intercalation of non-refractory metals and compounds including two-dimensional silver (2D-Ag) and gallium nitride (2D-GaN_x).

Introduction

Since its discovery >150 years ago, intercalation has enabled the creation of materials for applications ranging from catalysis and energy storage, to superconductivity and lubrication.[3–8] Importantly, intercalation also enables the decoupling of layers from bulk materials, as well as from native substrates.[9,10] For example, epitaxial graphene (EG) layers grown on silicon carbide (SiC) substrates may be physically decoupled from the substrate by intercalating species to the EG/SiC interface.[10] EG is created when Si atoms sublime from the surface of SiC, leaving behind carbon atoms which reconstruct epitaxially with the SiC surface. This process enables the realization of large-area graphene layers, but also results in the formation of a honeycomb, carbon buffer layer that is partially covalently bound to the SiC surface.[10] This buffer layer scatters carriers in overlying graphene, thereby decreasing carrier mobility compared to

exfoliated graphene.[11,12] Importantly, intercalation of atomic species to the buffer layer/SiC interface physically and electronically decouples the buffer layer from SiC, resulting in the formation of quasi-free standing epitaxial graphene (QFEG) layers with improved carrier transport.[13] This decoupling is possible using a wide range of intercalant species, including H, O, Ge, and Pd, among others.[10,14–21] While the precise mechanism of atomic intercalation to the EG/SiC interface is under active investigation, there is experimental evidence that the intercalant atoms diffuse through graphene defects and domain edges to reach to the EG/SiC interface.[2,10,16,22,23] In this review we discuss intercalation in EG/SiC systems, highlighting key techniques to realize intercalated EG/SiC materials, and emphasize the promise of intercalation to realize unique 2D materials and compounds.

Experimental Considerations for Intercalated Epitaxial Graphene

Experimental parameters play a significant role in achieving intercalation to the EG/SiC interface. Here we discuss key components of the EG intercalation process, including EG growth, surface treatments, precursors, and intercalation methods.

Epitaxial Graphene on Silicon Carbide: Growth and Characterization

While high-temperature graphitization of SiC was first demonstrated in the 1960s,[24] the experimental realization of graphene's unique properties in 2004[1,25] led to a resurgence in the technique for mono- to few-layer graphene growth.[1] Heating SiC substrates to temperatures above 1200°C[26] under pressures ranging from ultra-high vacuum,[24] to atmospheric[26] results in the sublimation of silicon atoms from the SiC surface, where remaining carbon undergoes a ($6\sqrt{3}$ x $6\sqrt{3}$)R30° reconstruction. This first carbon layer is commonly referred to as the buffer or zero layer, and consists of carbon atoms in a honeycomb structure, 1/3 of which are covalently bound to Si in the underlying SiC. Heating SiC substrates for increased time at elevated temperatures enables the formation of multiple graphene layers through continued sublimation of Si from SiC.[27]

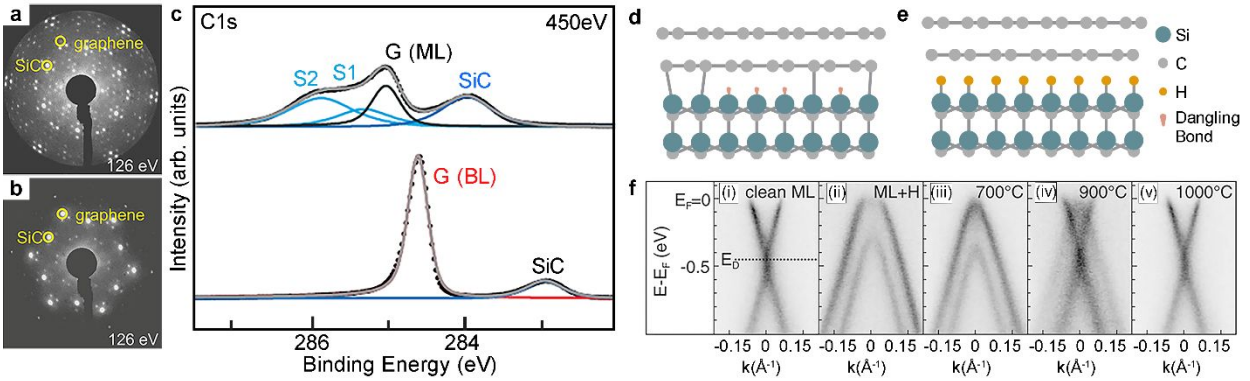

Figure 1: LEED patterns for buffer layer EG before (a) and after (b) hydrogen intercalation. Reconstruction spots are suppressed upon intercalation of hydrogen atoms. (c) C 1s core level spectra of monolayer graphene (buffer + 1 layer) before (top) and after (bottom) hydrogen intercalation, where hydrogen intercalation decouples the buffer layer, creating QFEG, as depicted in (d) and (e). Upon intercalation, the C 1s SiC peak shifts to lower binding energies and the buffer layer S1 and S2 components are no longer present. (f) ARPES measurements show the monolayer graphene (d) Dirac cone before (f, i) and after (f, ii) hydrogen intercalation. Deintercalation of hydrogen is observed as the sample is annealed and the Dirac point returns to its initial energy (f, iii-v). Images are reproduced from reference 10 with permission from the American Physical Society.

Identification and investigation of as-grown and intercalated EG layers on SiC is commonly performed through a variety of analytical techniques including low energy electron diffraction (LEED) (Figure 1a,b) and microscopy (LEEM), as well as x-ray photoelectron (XPS) (Figure 1c) and angle-resolved photoemission spectroscopies (ARPES). When investigating intercalation, low energy electron diffraction may be used to monitor the EG/SiC system as it progresses from its initial state, containing a ($6\sqrt{3}$ x $6\sqrt{3}$)R30° reconstructed (buffer) layer bonded to SiC (Figure 1a,d), to its final intercalated state, where the buffer layer is decoupled from the SiC and transformed to QFEG (Figure 1b,e).[28] Because the buffer layer exhibits a markedly different electron pattern from QFEG, the two structures may be easily distinguished (Figure 1a,b). The diffracted beam may also be used to image the material surface and acquire LEEM images. Such images enable identification of regions across sample surfaces containing QFEG versus as-grown EG. Furthermore, I-V electron reflectivity curves acquired via LEEM enable identification of the number of graphene layers present and additional changes in the EG/SiC interface. As a result, LEEM is a valuable technique to spatially identify and monitor intercalation.[10,15,29,30]

Apart from LEED and LEEM, changes in the C 1s and Si 2p core electron regions acquired from XPS can also indicate intercalation (Figure 1c). The C1s region of pristine EG/SiC exhibits features related to the buffer layer and bulk SiC, as well as any QFEG that may be present. Given sufficient energy resolution, the C 1s buffer layer component (Figure 1c) may be fitted with S1 and S2 peaks, where S1 corresponds to carbon atoms in the reconstructed buffer layer bound to one Si atom in SiC and 3 sp^2 C atoms within the buffer layer, and S2 corresponds to the remaining sp^2 C atoms in the reconstructed layer.[28,31] Intercalation of atoms to the EG/SiC interface eliminates the buffer layer component from the C 1s region, due to disruption of the buffer layer bonding to SiC. Additionally, a shift of approximately 0.7-2.0eV in bulk SiC C 1s and Si 2p peak positions is often observed in the XPS spectrum as a result of intercalation.[10,16,19,32–40] This shift indicates a change in the charge transfer between SiC and EG caused by the presence of an intercalant layer.

Changes in the doping of graphene layers can also signify intercalation. This can be investigated through ARPES, where the graphene Dirac point can be monitored relative to the Fermi level. Changes in the Dirac point following exposure of EG to intercalant species can indicate intercalation to the EG/SiC interface and decoupling of the buffer layer (Figure 1f).[10] Similarly, restoration of the Dirac point to its original energy following additional sample annealing can indicate deintercalation of atoms from the EG/SiC interface and reformation of the buffer layer (Figure 1f,v).[10] While practically absent from intercalation studies to-date, Auger electron spectroscopy and cross-sectional scanning transmission electron microscopy are two additional valuable techniques to directly investigate the surface and interfacial chemistry, as well as the structure of intercalated EG/SiC systems.[2,23] As the field progresses, these techniques should be considered key components for investigation and identification of intercalated materials, particularly when techniques such as LEEM are not accessible.

Defect-Mediated Intercalation

Epitaxial graphene readily accommodates intercalation.[15,16,19,20,41,42] Hydrogen intercalation – perhaps the most commonly studied case of EG/SiC intercalation – may be achieved by directly annealing as-grown EG/SiC in molecular hydrogen.[10,43] While hydrogen intercalation has been

demonstrated using multilayers of high-quality EG/SiC,[43] defective EG/SiC may also be used to achieve intercalation of a broad range of elements.[2,16,23] Defects in EG are believed to serve as windows through which atoms can access the EG/SiC interface, and may be native to the grown EG/SiC (for example, at EG grain boundaries and wrinkles[2,10]), or purposely introduced prior to or during intercalation.[2,16,23] For example, Li intercalation is hypothesized to be enabled by the formation of cracks and defects in graphene layers caused by initial deposition of Li on the EG surface.[16] For cases in which intercalation is not achievable using high-quality EG/SiC, defective EG may be used to promote intercalation over large areas.[23] For example, exposing EG layers to O_2/He plasmas can result in the formation of carbon vacancies, where vacancy edge atoms may also become passivated by plasma constituents. Passivated species such as C–O–C are believed to aid intercalation by binding to intercalant atoms more strongly than pristine graphene layers.[23] Thus, these passivated species can effectively draw intercalants to the graphene surface where intercalation can take place. Plasma-treated EG layers have purposely been used to realize large-area Ga, In, and Sn,[23] and GaN_x (via metal-organic chemical vapor deposition),[2] and as shown later in this manuscript, 2D-Ag and 2D-GaN_x via thermal evaporation.

Intercalation Approaches

A wide library of EG/SiC intercalants have been demonstrated over the last decade (Table 1), enabling p-type, n-type, as well as charge neutral graphene. Intercalated Ge and Au have been shown to enable both p and n type graphene doping individually, which is attributed to different thicknesses of the elemental layers at the EG/SiC interface. Most EG intercalations (Table 1) utilize an initial deposition step, where metal atoms (Co, Pt, Fe, and Au, for example) are deposited onto the EG surface via thermal or E-beam evaporation, sputtering, or molecular beam/Knudsen cell deposition.[20,32,39,42] Following this step, EG/SiC substrates are annealed at temperatures typically $\geq 600°C$ under ultra-high vacuum (UHV), to induce intercalation.[20,32,37,39,42] This synthesis approach is well suited to investigation of intercalated structures, due to the relative ease of characterizing samples *in situ* through techniques such as LEED, LEEM, ARPES, and XPS. Investigation of intercalated materials through scanning tunneling microscopy and spectroscopy is also common, and can reveal ordered intercalant structures underneath the graphene layers.[17,33,44–47]

Elemental intercalation may also be achieved using gas-phase precursors such as H_2, O_2, air, and NH_3.[2,10,18,36,37] In a similar fashion to metals deposited on EG, gas phase species are hypothesized to adsorb onto the graphene surface and diffuse through graphene layers. In contrast to typical UHV metal intercalation, intercalation of elements from gaseous precursors is typically performed near atmospheric pressure.[10,18,37,48] While less studied, alternative sources such as plasmas, metal-organics, molten baths, and molecular precursors may also enable intercalation.[2,14,49,50] Such sources have been successfully used to intercalate H, Ga, Ca and F. Overall, these studies demonstrate that a wide range of precursors and pressures may be used to achieve elemental intercalation.

While EG/SiC intercalation is most commonly performed in UHV, alternative approaches may also be used to achieve intercalated EG/SiC structures. For example, elemental intercalation and compound formation is possible at elevated pressures using metal-organic[2] or solid metallic precursors.[23] Solid precursors can be heated together with EG/SiC substrates in a tube furnace or sealed ampoule.[23,50] This simultaneous heating approach is effective for intercalating a wide

range of non-refractory metals with melting temperatures near or below ~900°C, which can be reached using a simple tube furnace. Heating at or above the melting temperatures of metallic precursors can yield vapor pressures great enough for intercalation. However, to intercalate high-melting temperature metals, the use of compound precursors may be necessary. In such cases, decomposition chemistry, relative constituent vapor pressure, and flow or vapor transport characteristics must also be considered in order to achieve intercalation.

Compound Formation at the EG/SiC Interface

Beyond 2D elemental layers, intercalation and reaction can enable interfacial, compound 2D materials. For example, compound materials such as Iron(II) oxide[51] and chromium carbide[52] have been achieved via intercalation through EG on metal substrates. In the case of EG/SiC systems, atomically-thin ytterbium oxide[53] and GaN_x[2] have been demonstrated by way of intercalation. Ytterbium oxide was achieved by intercalation of ytterbium and subsequent annealing in oxygen, whereas 2D GaN_x was achieved via Ga intercalation from trimethyl gallium, followed by reaction with NH_3.[2] An interfacial silicon-nitride structure has also been demonstrated between EG and SiC, although this layer was achieved by annnealing SiC in N_2/Ar prior to EG growth.[54] These studies demonstrate that a wide array of materials and chemistries can be achieved between EG and SiC, and further reveal the promise of material interfaces in realizing 2D forms of bulk materials. Furthermore, the properties of these artificially confined materials differ from the bulk, as demonstrated in the initial 2D GaN_x report by Al Balushi *et al.*, which shows that 2D GaN_x exhibits dramatically different electronic and atomic structures compared to bulk GaN. These findings further indicate that 2D interfacial compounds are unique from their bulk counterparts.

Intercalant	Intercalation Pressure	Intercalation Temperature (°C)	Deintercalation Temperature (°C)	Majority Carrier Type	E_D relative to E_f (E_f=0) (meV)
H	600 Torr[13] atmospheric[10]	600 – 1200[10,13]		p	100[10]
Li	UHV[35,55]	290 – 330[16] 350[55] 360[35]	500[55]	n	-650 – -900[16] -1000[55] -1400[35]
N		500[36]			
O	Atmospheric[18,37,48,56]	250[18,56] 600[37,48] 750[56]		p	
F		200[57] 800[14]	1200[14]	p[57] neutral[14]	790[57] 0[14]
Na	UHV[58]	180[58]		n	
Si	UHV	750[38] 800[59]	1000[38,59]	n	-260[38] -300[59]
Ca		350[50]			
Mn	UHV	600[60]	1200[60]	n	-300[60]
Fe	UHV	600[39]		n	-250[39]
Co	UHV	650 – 800[17,42]			
Cu	UHV	600[41] 700[21]	800[41]	n	900[41] 850[21]
Ga	50 Torr	550, 675[2]			
GaN_x	50 Torr	550, 675[2]			
Ge	UHV	720[15]	800[15]	p, n	
Pd	UHV	>700[19]	900[19]	neutral	
Sn	UHV	850[40]	1050[40]		
Eu	UHV	800[61] 120 – 300[62]	1050[62]	n	
Yb	UHV[53]	500[53]		n	1500[53]
YbO_x	UHV	500, 260[53]		n	400[53]
Pt	UHV	900[32]		n	-150[32]
Au	UHV[20,44,63]	800 – 1000[20,44,63]		p[20], n[20,63]	100[20] -232[63] -850[20]
Pb	UHV	675[33]		p	100[33]

Table 1: EG/SiC Intercalation Conditions (Temperature, Pressure) and Resulting Graphene Carrier Type

Intercalation via Thermal Vaporization: Creating 2D Silver and GaN_x

Silver is a promising material for plasmon-based technologies such as biosensors and waveguides.[64–69] However, implementation of Ag films into plasmonic devices is limited by the need for encapsulation layers that can protect Ag films from degradation. Intercalation of Ag atoms through EG layers is one promising method to realize Ag films with an inherent, overlying graphene capping layer.[70,71] While intercalation of Ag through graphene on native metal substrates has been performed with mixed success,[72–74] we show that EG/SiC may be reliably intercalated with Ag to realize encapsulated, 2D-Ag films for plasmonic applications.

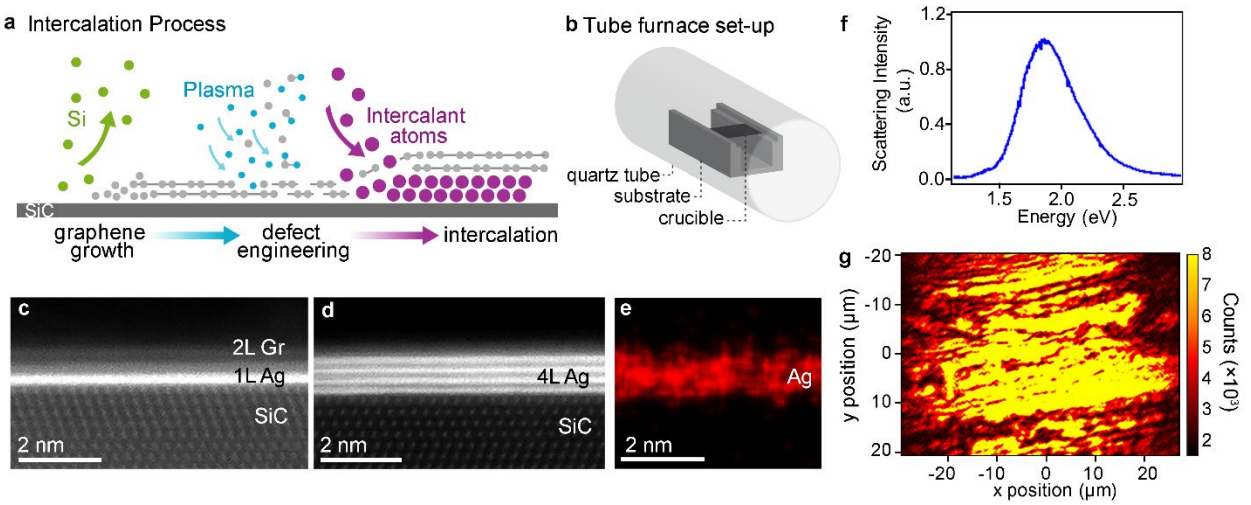

Figure 2: (a) Intercalation schematic illustrating graphene growth, plasma treatment, and metal intercalation (b) Diagram of experimental setup depicting a quartz tube containing an alumina crucible and an EG/SiC substrate placed facing downward on the crucible over the metal source. (c) Cross-sectional STEM showing 1 and (d) 4 layers of Ag between EG and SiC. (e) Corresponding Ag EDS. (f) Dark field scattering spectrum showing a peak at 1.87 eV, reflecting the plasmonic character of the Ag film. (g) Map of SHG peak across the EG/Ag/SiC surface showing the presence of Ag layers across 10s of microns.

2D-Ag films are synthesized using the process detailed in Figure 2a, where EG is first synthesized on the Si face of SiC.[75] Following this synthesis, defects in the EG layers are generated by exposing EG to an O_2/He plasma treatment.[23] EG/SiC substrates are then placed face down over metallic Ag powder and heated to 900-950°C, under 300 Torr Ar for 20 minutes (Figure 2b). A constant flow rate of 50 sccm Ar is maintained throughout the synthesis period. Cross-sectional scanning transmission electron microscopy (STEM) of intercalated Ag samples shows 1 and 4 Ag layers located between graphene and the SiC substrate (Figure 2c,d). These interfacial layers are confirmed to consist of Ag atoms through energy dispersive x-ray spectroscopy mapping (EDS) (Figure 2e). Dark-field microscopy and second harmonic generation (SHG) imaging measurements are performed to investigate the plasmonic properties of 2D-Ag. The normalized dark-field scattering spectrum in Figure 2f shows a peak at 1.87 eV which reveals that the intercalated Ag film exhibits a plasmon resonance in the visible region. The same measurements are performed on a 40 nm, bare Ag film directly deposited on SiC via electron beam evaporation. Unlike the intercalated Ag, the deposited film does not exhibit any dark field spectral peak, possibly due to degradation of the Ag film during transportation of the sample and measurement in ambient.[76–78] Thus, intercalation of Ag atoms to the EG/SiC interface is a promising approach for protection of metal films from degradation.

Second harmonic generation imaging microscopy (Figure 2g) confirms that 2D-Ag created at the EG/SiC interface supports non-linear optical phenomena with uniform responses over large areas. Decreased intensity observed near the edges of the image is attributed to the point-spread function of the optical setup utilized for the measurement. However, the stripe-like pattern is the result of 2D-Ag discontinuities that result from large (>2 nm) steps in the SiC substrate. This demonstrates that even with uniform defect formation in EG prior to intercalation, the SiC morphology can play a significant role in achieving uniform elemental intercalation. The nonlinear optical enhancement observed via SHG measurements further supports the notion that intercalated Ag layers exist in a metallic, plasmon-supporting state and are protected from degradation by overlying graphene.[79,80] The SHG measurements also enable extraction of the second order non-linear susceptibility (χ^2) of 2D-Ag. In the case of 2D-Ag formed via intercalation, $\chi^2 \approx 1.7 \times 10^{-9}$ m/V, which is 250 × larger than that of Ag nanoparticle colloids.[81] The large increase in χ^2 is attributed to a combination of plasmon-resonant excitation and the non-symmetric bonding that occurs in 2D metals intercalated at the interface of EG and SiC[23] that enables large second-order non-linear responses. Therefore, the creation of 2D-Ag constitutes a major advancement in the use of Ag films in practical photonic applications.

The rudimentary thermal-evaporation process introduced for Ag intercalation can also provide access to novel compound materials at the EG/SiC interface, and can do so without significant infrastructure requirements. Here, we show that the tube furnace thermal-evaporation process enables the formation of 2D GaN_x. The process is identical to that outlined in Figures 2a and 2b, except that intercalation and reaction is performed at 700°C. Following synthesis, samples are characterized via cross-sectional STEM, EDS, and electron energy loss spectroscopy (EELS) (Figure 3a-e). Figures 3a and 3b show cross-sectional STEM of two regions, showing the Ga bilayer along with few nanometer thick GaN located between EG and SiC. This is consistent with previously reported 2D-GaN_x.[2] Both 2D-GaN_x and the bulk-like GaN show N and Ga signatures from EDS and EELS measurements (Figure 3c,d,e). These results demonstrate that intercalation at the EG/SiC interface is a robust phenomenon accessible via multiple deposition techniques.

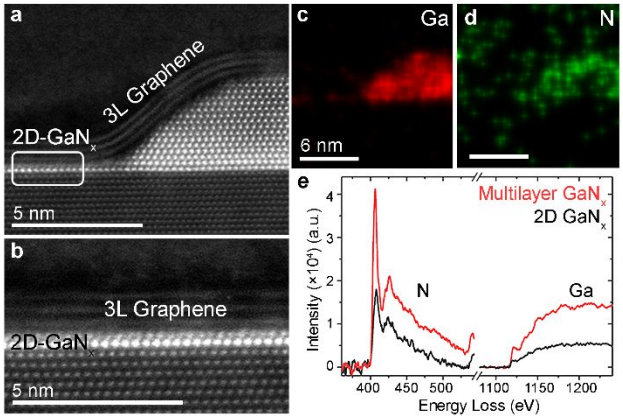

Figure 3: (a, b) Cross-sectional STEM showing 2D and multilayer GaN_x between EG and SiC. (c,d) EDS maps of Ga and N for the multilayer region shown in (a). (e) EELS spectra for GaN_x in (a,b) showing N and Ga signatures from both regions.

Conclusion and Outlook

Over the last decade, EG/SiC intercalation has been demonstrated under UHV and atmospheric conditions using a variety of precursor materials. Recent studies emphasize the importance of graphene defects in achieving large-area intercalation. We demonstrate a simplified approach to realizing EG/metal/SiC structures, which utilizes thermal evaporation of metal sources at $\geq$ 300 Torr. This method yields large-area, plasmonically-active metal layers which are protected from environmental effects. Looking forward, intercalation and reaction at the EG/SiC interface may

be adopted to realize a wide-array of 2D systems not previously considered due to thermodynamic and kinetic limitations. Overall, EG/SiC intercalation can enable the realization of 2D forms of materials that do not exist in nature, and which hold promise for a variety of technologies. In future studies, 2D layers and bulk substrates beyond graphene and SiC may be investigated as host systems to enable new, interfacial 2D layers.

Acknowledgements
The authors thank Z.Y. Al Balushi and J.M. Redwing for insightful comments regarding compound formation at the EG/SiC interface. This work was supported in part by the 2D Crystal Consortium National Science Foundation (NSF) Materials Innovation Platform under cooperative agreement DMR-1539916, Northrop Grumman Mission Systems' University Research Program, the Semiconductor Research Corporation Intel/Global Research Collaboration Fellowship, task 2741.001, a grant from the Air Force Office of Scientific Research, grant number FA-9550-18-1-0347, and the NSF CAREER award 1453924.

References

1. Berger, C. *et al.* Ultrathin Epitaxial Graphite: 2D Electron Gas Properties and a Route toward Graphene-based Nanoelectronics. *J. Phys. Chem. B* **108**, 19912–19916 (2004).
2. Al Balushi, Z. Y. *et al.* Two-dimensional gallium nitride realized via graphene encapsulation. *Nat. Mater.* **15**, 1166–1171 (2016).
3. Boersma, M. A. M. Catalytic properties of alkali metal-graphite intercalation compounds. *Catal. Rev.* **10**, 243–280 (1974).
4. Brodie, B. C. XIII . On the atomic weight of graphite. *Philos. Trans. R. Soc. London* **149**, 249–259 (1859).
5. Schafhaeutl, C. Ueber die Verbindungen des Kohlenstoffes mit Silicium, Eisen und anderen Metallen, welche die verschiedenen Gallungen von Roheisen, Stahl und Schmiedeeisen bilden. *J. fuer Prakt. Chemie* **21**, 129–157 (1840).
6. Dresselhaus, M. S. & Dresselhaus, G. Intercalation compounds of graphite. *Adv. Phys.* **30**, 139–326 (1981).
7. Ebert, L. B. Catalysis by graphite intercalation compounds. *J. Mol. Catal.* **15**, 275–296 (1982).
8. Enoki, T., Suzuki, M. & Endo, M. *Graphite intercalation compounds and applications*. (Oxford University Press, 2003).
9. Zhang, Z. & Lerner, M. M. Preparation, Characterization, and Exfoliation of Graphite Perfluorooctanesulfonate. *Chem. Mater.* **8**, 257–263 (1996).
10. Riedl, C., Coletti, C., Iwasaki, T., Zakharov, A. A. & Starke, U. Quasi-Free-Standing Epitaxial Graphene on SiC Obtained by Hydrogen Intercalation. *Phys. Rev. Lett.* **103**, 246804 (2009).
11. Bolotin, K. I. *et al.* Ultrahigh electron mobility in suspended graphene. *Solid State Commun.* **146**, 351–355 (2008).
12. Jobst, J. *et al.* Quantum oscillations and quantum Hall effect in epitaxial graphene. *Phys. Rev. B* **81**, 195434 (2010).
13. Robinson, J. A. *et al.* Epitaxial Graphene Transistors: Enhancing Performance via Hydrogen. *Nano Lett.* **11**, 3875–3880 (2011).
14. Wong, S. L. *et al.* Quasi-Free-Standing Epitaxial Graphene on SiC (0001) by Fluorine Intercalation from a Molecular Source. *ACS Nano* **5**, 7662–7668 (2011).
15. Emtsev, K. V, Zakharov, A. A., Coletti, C., Forti, S. & Starke, U. Ambipolar doping in quasifree epitaxial graphene on SiC (0001) controlled by Ge intercalation. *Phys. Rev. B* **84**, 125423 (2011).
16. Virojanadara, C., Watcharinyanon, S., Zakharov, A. A. & Johansson, L. I. Epitaxial graphene on 6H-SiC and Li intercalation. *Phys. Rev* **82**, 205402 (2010).
17. de Lima, L. H., Landers, R. & de Siervo, A. Patterning Quasi-Periodic Co 2D-Clusters underneath

Graphene on SiC(0001). *Chem. Mater.* **26**, 4172–4177 (2014).
18. Oida, S. *et al.* Decoupling graphene from SiC(0001) via oxidation. *Phys. Rev. B - Condens. Matter Mater. Phys.* **82**, 041411(R) (2010).
19. Yagyu, K., Takahashi, K., Tochihara, H., Tomokage, H. & Suzuki, T. Neutralization of an epitaxial graphene grown on a SiC (0001) by means of palladium intercalation. *Appl. Phys. Lett.* **110**, 131602 (2017).
20. Gierz, I. *et al.* Electronic decoupling of an epitaxial graphene monolayer by gold intercalation. *Phys. Rev. B - Condens. Matter Mater. Phys.* **81**, 235408 (2010).
21. Forti, S. *et al.* Mini-Dirac cones in the band structure of a copper intercalated epitaxial graphene superlattice. *2D Mater.* **3**, 035003 (2016).
22. Markevich, A. *et al.* First-principles study of hydrogen and fluorine intercalation into graphene-SiC(0001) interface. *Phys. Rev. B - Condens. Matter Mater. Phys.* **86**, 045453 (2012).
23. Briggs N. & Bersch B. *et al.* Confinement Heteroepitaxy: Realizing Atomically Thin, Half-van der Waals Materials. *http://arxiv.org/abs/1905.09962* (2019).
24. Badami, D. V. Graphitization of α-Silicon Carbide. *Nature* **193**, 569–570 (1962).
25. Novoselov, K. S. *et al.* Electric field effect in atomically thin carbon films. *Science* **306**, 666–669 (2004).
26. Emtsev, K. V. *et al.* Towards wafer-size graphene layers by atmospheric pressure graphitization of silicon carbide. *Nat. Mater.* **8**, 203–207 (2009).
27. Riedl, C., Coletti, C. & Starke, U. Structural and electronic properties of epitaxial Graphene on SiC(0001): A review of growth, characterization, transfer doping and hydrogen intercalation. *J. Phys. D. Appl. Phys.* **43**, 374009 (2010).
28. Riedl, C. Epitaxial Graphene on Silicon Carbide Surfaces: Growth, Characterization, Doping and Hydrogen Intercalation. *Ph.D. Friedrich-Alexander-Universität Erlangen-nürnb.* 1–173 (2010).
29. Hibino, H. *et al.* Microscopic thickness determination of thin graphite films formed on SiC from quantized oscillation in reflectivity of low-energy electrons. *Phys. Rev. B* **77**, 075413 (2008).
30. Emtsev, K. V *et al.* Towards wafer-size graphene layers by atmospheric pressure graphitization of silicon carbide. *Nat. Mater.* **8**, 203–207 (2009).
31. Emtsev, K. V., Speck, F., Seyller, T., Ley, L. & Riley, J. D. Interaction, growth, and ordering of epitaxial graphene on SiC{0001} surfaces: A comparative photoelectron spectroscopy study. *Phys. Rev. B* **77**, 155303 (2008).
32. Xia, C., Johansson, L. I., Niu, Y., Zakharov, A. A. & Janze, E. High thermal stability quasi-free-standing bilayer graphene formed on 4H-SiC(0001) via platinum intercalation. *Carbon N. Y.* **79**, 631–635 (2014).
33. Yurtsever, A., Onoda, J., Iimori, T., Niki, K. & Miyamachi, T. Effects of Pb Intercalation on the Structural and Electronic Properties of Epitaxial Graphene on SiC. *Small* **12**, 3956–3966 (2016).
34. Sieber, N. *et al.* Synchrotron x-ray photoelectron spectroscopy study of hydrogen-terminated 6H-SiC{0001} surfaces. *Phys. Rev. B* **67**, 205304 (2003).
35. Bisti, F. *et al.* Electronic and geometric structure of graphene / SiC (0001) decoupled by lithium intercalation. **91**, 245411 (2015).
36. Wang, Z. *et al.* Simultaneous N-intercalation and N-doping of epitaxial graphene on 6H-SiC (0001) through thermal reactions with ammonia. *Nano Res.* **6**, 399–408 (2013).
37. Oliveira, M. H. *et al.* Formation of high-quality quasi-free-standing bilayer graphene on SiC (0001) by oxygen intercalation upon annealing in air. *Carbon N. Y.* **52**, 83–89 (2012).
38. Silly, M. G. *et al.* Electronic and structural properties heterostructures engineered by silicon intercalation. *Carbon N. Y.* **76**, 27039 (2014).
39. Sung, S. J. *et al.* Spin-induced band modifications of graphene through intercalation of magnetic iron atoms. *Nanoscale* **6**, 3824–3829 (2014).
40. Kim, H., Dugerjav, O. & Lkhagvasuren, A. Charge neutrality of quasi-free-standing monolayer graphene induced by the intercalated Sn layer. *J. Phys. D. Appl. Phys.* **49**, 135307 (2016).

41. Yagyu, K. *et al.* Fabrication of a single layer graphene by copper intercalation on a SiC(0001) surface. *Appl. Phys. Lett.* **104**, 053115 (2014).
42. Zhang, Y., Zhang, H., Cai, Y., Song, J. & He, P. The investigation of cobalt intercalation underneath epitaxial graphene on 6H-SiC(0 0 0 1). *Nanotechnology* **28**, 075701 (2017).
43. Coletti, C. *et al.* Revealing the electronic band structure of trilayer graphene on SiC: An angle-resolved photoemission study. *Phys. Rev. B* **88**, 155439 (2013).
44. Premlal, B. *et al.* Surface intercalation of gold underneath a graphene monolayer on SiC(0001) studied by scanning tunneling microscopy and spectroscopy. *Appl. Phys. Lett.* **94**, 263115 (2009).
45. Cranney, M. *et al.* Superlattice of resonators on monolayer graphene created by intercalated gold nanoclusters. *EPL Europhys. Lett.* **91**, 66004 (2010).
46. Nair, M. N. *et al.* High van Hove singularity extension and Fermi velocity increase in epitaxial graphene functionalized by intercalated gold clusters. *Phys. Rev. B* **85**, 263115 (2012).
47. Zhang, Y., Zhang, H., Cai, Y., Song, J. & He, P. The investigation of cobalt intercalation underneath epitaxial graphene on 6H-SiC(0 0 0 1). *Nanotechnology* **28**, 075701 (2017).
48. Kowalski, G., Tokarczyk, M., Ciepielewski, P. & Baranowski, J. M. New X-ray insight into oxygen intercalation in epitaxial graphene grown on 4 H -SiC (0001). *J. Appl. Phys.* **117**, 105301 (2017).
49. Virojanadara, C., Zakharov, A. A., Yakimova, R. & Johansson, L. I. Buffer layer free large area bi-layer graphene on SiC(0 0 0 1). *Surf. Sci.* **604**, L4–L7 (2010).
50. Li, K. *et al.* Superconductivity in Ca-intercalated epitaxial graphene on silicon carbide. *Appl. Phys. Lett.* **103**, 062601 (2013).
51. Dahal, A. & Batzill, M. Growth from behind: Intercalation-growth of two-dimensional FeO moiré structure underneath of metal-supported graphene. *Sci. Rep.* **5**, 11378 (2015).
52. Caffrey, N. M., Armiento, R., Yakimova, R. & Abrikosov, I. A. Charge neutrality in epitaxial graphene on 6H-SiC(0001) via nitrogen intercalation. *Phys. Rev. B* **92**, 081409(R) (2015).
53. Watcharinyanon, S., Johansson, L. I., Xia, C. & Virojanadara, C. Ytterbium oxide formation at the graphene–SiC interface studied by photoemission. *J. Vac. Sci. Technol. A Vacuum, Surfaces, Film.* **31**, 020606 (2013).
54. Masuda, Y., Norimatsu, W. & Kusunoki, M. Formation of a nitride interface in epitaxial graphene on SiC (0001). *Phys. Rev. B* **91**, 075421 (2015).
55. Virojanadara, C., Zakharov, A. A., Watcharinyanon, S., Yakimova, R. & Johansson, L. I. A low-energy electron microscopy and x-ray photo-emission electron microscopy study of Li intercalated into graphene on SiC(0001). *New J. Phys.* **12**, 125015 (2010).
56. Ostler, M. *et al.* Decoupling the Graphene Buffer Layer from SiC(0001) via Interface Oxidation. *Mater. Sci. Forum* **717–720**, 649–652 (2012).
57. Walter, A. L. *et al.* Highly p-doped epitaxial graphene obtained by fluorine intercalation. *Appl. Phys. Lett.* **98**, 184102 (2011).
58. Sandin, A. *et al.* Multiple coexisting intercalation structures of sodium in epitaxial graphene-SiC interfaces. *Phys. Rev. B* **85**, 125410 (2012).
59. Xia, C. *et al.* Si intercalation/deintercalation of graphene on 6H-SiC(0001). *Phys. Rev. B* **85**, 045418 (2012).
60. Gao, T. *et al.* Atomic-Scale Morphology and Electronic Structure of Manganese Atomic Layers Underneath Epitaxial Graphene on SiC (0001). *ACS Nano* **6**, 6562–6568 (2012).
61. Anderson, N. A., Hupalo, M., Keavney, D., Tringides, M. C. & Vaknin, D. Intercalated europium metal in epitaxial graphene on SiC. *Phys. Rev. Mater.* **1**, 054005 (2017).
62. Sung, S. *et al.* Observation of variable hybridized-band gaps in Eu-intercalated graphene. *Nanotechnology* **28**, 205201 (2017).
63. Nair, M. N. *et al.* High van Hove singularity extension and Fermi velocity increase in epitaxial graphene functionalized by intercalated gold clusters. *Phys. Rev. B* **85**, 245421 (2012).
64. Johnson, P. B. & Christy, R. W. Optical Constants of the Noble Metals. *Phys. Rev. B* **6**, 4370–

4379 (1972).
65. Tsuda, Y., Omoto, H., Tanaka, K. & Ohsaki, H. The underlayer effects on the electrical resistivity of Ag thin film. *Thin Solid Films* **502**, 223–227 (2006).
66. Anker, J. N. *et al.* Biosensing with plasmonic nanosensors. *Nat. Mater.* **7**, 442–453 (2008).
67. Simon, H. J., Mitchell, D. E. & Watson, J. G. Optical Second-Harmonic Generation with Surface Plasmons in Silver Films. *Phys. Rev. Lett.* **33**, 1531–1534 (1974).
68. Quail & Simon. Second-harmonic generation from silver and aluminum films in total internal reflection. *Phys. Rev. B* **31**, 4900–4905 (1985).
69. Oulton, R. F., Sorger, V. J., Genov, D. A., Pile, D. F. P. & Zhang, X. A hybrid plasmonic waveguide for subwavelength confinement and long-range propagation. *Nat. Photonics* **2**, 496–500 (2008).
70. Losurdo, M. *et al.* Graphene as an Electron Shuttle for Silver Deoxidation: Removing a Key Barrier to Plasmonics and Metamaterials for SERS in the Visible. *Adv. Funct. Mater.* **24**, 1864–1878 (2014).
71. Hong, H. Y., Ha, J. S., Lee, S.-S. & Park, J. H. Effective Propagation of Surface Plasmon Polaritons on Graphene-Protected Single-Crystalline Silver Films. *ACS Appl. Mater. Interfaces* **9**, 5014–5022 (2017).
72. Tontegode, A. Y. & Rut'kov, E. V. Intercalation by atoms of a two-dimensional graphite film on a metal. *Physics-Uspekhi* **36**, 1053–1067 (1993).
73. Starodubov, A. G., Medvetskii, M. A., Shikin, A. M. & Adamchuk, V. K. Intercalation of silver atoms under a graphite monolayer on Ni(111). *Phys. Solid State* **46**, 1340–1348 (2004).
74. Farías, D., Shikin, A. M., Rieder, K.-H. & Dedkov, Y. S. Synthesis of a weakly bonded graphite monolayer on Ni(111) by intercalation of silver. *J. Phys. Condens. Matter* **11**, 8453–8458 (1999).
75. Subramanian, S. *et al.* Properties of synthetic epitaxial graphene/molybdenum disulfide lateral heterostructures. *Carbon N. Y.* **125**, 551–556 (2017).
76. Han, Y. *et al.* Effect of Oxidation on Surface-Enhanced Raman Scattering Activity of Silver Nanoparticles: A Quantitative Correlation. *Anal. Chem.* **83**, 5873–5880 (2011).
77. Oates, T. W. H., Losurdo, M., Noda, S. & Hinrichs, K. The effect of atmospheric tarnishing on the optical and structural properties of silver nanoparticles. *J. Phys. D. Appl. Phys.* **46**, 145308 (2013).
78. Wang, X., Santschi, C. & Martin, O. J. F. Strong Improvement of Long-Term Chemical and Thermal Stability of Plasmonic Silver Nanoantennas and Films. *Small* **13**, 1700044 (2017).
79. Hong, H. Y., Ha, J. S., Lee, S.-S. & Park, J. H. Effective Propagation of Surface Plasmon Polaritons on Graphene-Protected Single-Crystalline Silver Films. *ACS Appl. Mater. Interfaces* **9**, 5014–5022 (2017).
80. Kravets, V. G. *et al.* Graphene-protected copper and silver plasmonics. *Sci. Rep.* **4**, 5517 (2015).
81. Kityk, I. V *et al.* Nonlinear optical properties of Au nanoparticles on indium–tin oxide substrate. *Nanotechnology* **16**, 1687–1692 (2005).

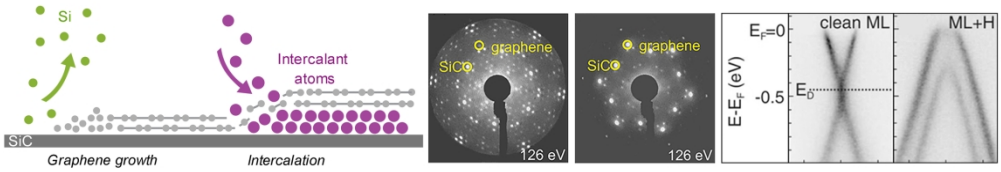

200x35mm (300 x 300 DPI)